Diseases of the Esophagus (2016) **29**, 307–313
DOI: 10.1111/dote.12317

DISEASES OF THE ESOPHAGUS

ISDE The International Society for Diseases of the Esophagus

Original article

Three-dimensional telomere architecture of esophageal squamous cell carcinoma: comparison of tumor and normal epithelial cells

S. Sunpaweravong,[1,2] P. Sunpaweravong,[1,3] C. Sathitruangsak,[1,3] S. Mai[1]

[1]*Genomic Center for Cancer Research and Diagnosis, Manitoba Institute of Cell Biology, University of Manitoba, Winnipeg, Manitoba, Canada; and Departments of* [2]*Surgery and* [3]*Internal Medicine, Faculty of Medicine, Prince of Songkla University, Songkla, Thailand*

SUMMARY. **Telomeres are repetitive nucleotide sequences (TTAGGG)n located at the ends of chromosomes that function to preserve chromosomal integrity and prevent terminal end-to-end fusions. Telomere loss or dysfunction results in breakage–bridge–fusion cycles, aneuploidy, gene amplification and chromosomal rearrangements, which can lead to genomic instability and promote carcinogenesis. Evaluating the hypothesis that changes in telomeres contribute to the development of esophageal squamous cell carcinoma (ESCC) and to determine whether there are differences between young and old patients, we compared the three-dimensional (3D) nuclear telomere architecture in ESCC tumor cells with that of normal epithelial cells obtained from the same patient. Patients were equally divided by age into two groups, one comprising those less than 45 years of age and the other consisting of those over 80 years of age. Tumor and normal epithelial cells located at least 10 cm from the border of the tumor were biopsied in ESCC patients. Hematoxylin and eosin staining was performed for each sample to confirm and identify the cancer and normal epithelial cells. This study was based on quantitative 3D fluorescence *in situ* hybridization (Q-FISH), 3D imaging and 3D analysis of paraffin-embedded slides. The 3D telomere architecture data were computer analyzed using 100 nuclei per slide. The following were the main parameters compared: the number of signals (number of telomeres), signal intensity (telomere length), number of telomere aggregates, and nuclear volume. Tumor and normal epithelial samples from 16 patients were compared. The normal epithelial cells had more telomere signals and higher intensities than the tumor cells, with *P*-values of $P < 0.0001$ and $P = 0.0078$, respectively. There were no statistically significant differences in the numbers of telomere aggregates or the nuclear volumes between the tumor and normal epithelial cells. Secondary analyses examined the effects of age on 3D telomere architecture and found no statistically significant differences in any parameter tested between the young and old patients in either the tumor or epithelial cells. The 3D nuclear telomeric signature was able to detect differences in telomere architecture between the ESCC and normal epithelial tissues. However, there were no differences observed between the young and old patients.**

KEY WORDS: **3D quantitative nuclear telomere analysis, esophageal cancer, Q-FISH, squamous cell carcinoma, telomere.**

INTRODUCTION

Esophageal cancer is the eighth most common cancer worldwide and ranks sixth among all cancers in terms of mortality.[1,2] Squamous cell carcinoma is the major type of this cancer, which arises in the esophageal epithelial cell layer.

Telomeres are repetitive nucleotide sequences (TTAGGG)n located at the ends of chromosomes that are capped by a protective protein complex termed shelterin.[3] Proper telomere capping preserves chromosomal integrity and prevents terminal end-to-end fusion. Telomere loss or dysfunction results in breakage–bridge–fusion cycles, aneuploidy, chromosomal rearrangements and gene amplification.[4] These events ultimately lead to genomic instability and promote carcinogenesis.[5]

Telomeres shorten with each cycle of cell division. Once they reach a critically short length, the cell normally undergoes senescence.[6] Therefore, rapidly dividing cells, such as tumor cells, often activate telomere lengthening mechanisms to survive.[7] Approximately 85% of tumor cells use telomerase, which is a reverse transcriptase with an RNA

Address correspondence to: Dr Somkiat Sunpaweravong, MD, Department of Surgery, Faculty of Medicine, Prince of Songkla University, Hat Yai, Songkla 90110, Thailand.
Email: susomkia@medicine.psu.ac.th

template, to add telomeres.[8] In contrast, approximately 15% of tumor cells use alternative lengthening of telomeres (ALT) mechanisms, which act through cycles of homologous recombination.[9]

The three-dimensional (3D) nuclear organization of telomeres allows for a distinction between normal and tumor cells. The nuclei of the latter tend to be disorganized and contain telomeric aggregates.[10] Alterations in telomere architecture are associated with the onset of genomic instability.[11–14] Our previous studies have shown altered 3D telomeric organization in different types of cancer.[4,10,12–20]

However, despite several studies showing the role of telomere dysfunction in the occurrence of malignancies, little is known about its possible role(s) in the evolution of esophageal squamous cell carcinoma (ESCC). In this study, we have, for the first time, examined and compared the 3D nuclear telomere architecture of invasive ESCC and normal epithelial cells using 3D quantitative fluorescence *in situ* hybridization (Q-FISH). We also evaluated a potential role of the ALT in ESCC.

MATERIALS AND METHODS

Patients

This study received approval by the research ethics board on human studies at the Faculty of Medicine, Prince of Songkla University. A total of 16 nonconsecutive patients with primary locally advanced (T3–4, N0, M0 any of T, N1, M0) ESCC who underwent treatment at the Prince of Songkla University Hospital in southern Thailand from January to December 2011 were enrolled. Patients were equally divided by age into two groups, including a young age group (under 45 years old) and old age group (over 80 years old). All specimens were obtained from patients by endoscopic biopsy of the esophagus prior to treatment with informed consent. Diagnosis of ESCC was histopathologically confirmed by pathologists. Specimens from each patient were retrieved from the two following sites: (i) the tumor site and (ii) the normal epithelial sites, which were located at least 10 cm from the border of the tumor. Hematoxylin and eosin staining was performed for each sample to confirm and identify the cancer and normal epithelial cells.

3D Q-FISH

The Q-FISH procedure was carried out on paraffin-embedded slides as a reference.[21] Briefly, after incubation in 3.7% formaldehyde/1× Phosphate Buffered Saline (PBS) for 20 minutes, the slides were immersed in 20% glycerol/1× PBS for 1 hour. Then, nuclei were treated with four repeated freeze–thaw cycles in glycerol/liquid nitrogen. Next, the slides were equilibrated in 0.1 HCl solution and fixed in 70% formamide/2× SCC for at least 1 hour. Immediately after this fixation step, 8 mL of Peptide Nucleic Acid (PNA) telomeric probe (DAKO, Mississauga, ON, Canada) was applied to the slides, which were sealed and placed into a Hybrite (Vysis; Abbott Diagnostics, Des Plaines, IL). Denaturation was carried out at 80°C for 3 minutes for both the cells and probe, after which hybridization was performed at 30°C for 2 hours. The slides were then washed twice for 15 minutes in 70% formamide/10 mmol/L Tris pH 7.4 followed by a washing step in 1× PBS at room temperature for 1 minute with shaking and in 0.1 × SSC at 55°C for 5 minutes with shaking. Next, the slides were washed in 2 × SSC/0.05% Tween 20 twice for 5 minutes each at room temperature with shaking. Thereafter, they were counterstained with 4',6-diamino-2-phenylindole (DAPI; 0.1 mg/mL) and coverslipped with ProLong GOLD antifade reagent (Invitrogen, Carlsbad, CA; Molecular probes) before image acquisition.

Image acquisition and 3D image analysis

3D image analysis was carried out on 100 nuclei per slide using an AxioImager Z1 microscope (Carl Zeiss Canada Ltd., Toronto, ON, Canada) and an AxioCam HRm charge-coupled device (Carl Zeiss Canada Ltd.). A 63 × oil objective lens (Carl Zeiss Canada Ltd.) was used at acquisition times of 300 milliseconds for Cy3 (telomeres) and 7 milliseconds for DAPI (nuclei). Forty z-stacks were acquired at a sampling distance of x,y: 102 nm and z: 200 nm for each slice of the stack. AxioVision 4.8 software (Carl Zeiss Canada Ltd.) was used for 3D image acquisition, and a constrained iterative algorithm was used for deconvolution. Deconvolved images were converted into Tagged Image File Format (TIFF) files and exported for 3D analysis using TeloView™ software.[22,23]

Data analysis

TeloView computed the following four parameters for each sample:

1 the number of signals, indicating the number of telomeres;
2 the signal intensity, representing the telomere length;
3 the number of telomere aggregates, indicating the number of telomere clusters that were in close proximity and could not be further resolved as separate entities by TeloView at an optical resolution limit of 200 nm; and
4 the nuclear volume.

These parameters in a 3D nucleus define all 3D telomere features that were measured. The following three types of histograms were produced:

1 line graphs showing the distribution of the intensity of the acquired telomere fluorescence signals;
2 histograms of the distribution of the number of aggregates per cell; and
3 histograms of the distribution of the number of acquired signals per cell. The percentage of cells with telomeric aggregates, the mean number of signals and the mean number of aggregates per cell were calculated. The histogram data from the different samples were combined into a single chart for comparison.

Immunohistochemistry (IHC) for ALT

A promyelocytic leukemia (PML) primary antibody (Abcam, ab53773, Cambridge, MA, USA; at a concentration of 4 μg/mL) and an anti-rabbit secondary antibody were used for IHC analysis. At least 200 cells from at least three different positions within each tumor were analyzed. ALT-associated PML protein nuclear body (APB)-positivity was determined based on PML signal. A positive control osteosarcoma cell line, U2OS, was stained by IHC as described in addition to negative control slides (which did not include primary antibody).[24,25]

Statistical considerations

A total of 16 patients were defined on the basis of their 3D telomeric profiles. The differences in the telomeric parameters (number, length, telomere aggregates and nuclear volume) between the tumor and the normal epithelial cells were compared among these 16 patients using nested factorial analysis of variance (ANOVA). Multiple pairwise comparisons using least square mean tests followed the significant omnibus subgroup effects. The significance level was set to $\alpha = 0.05$.

RESULTS

To investigate the 3D nuclear telomere architecture of ESCC, 3D Q-FISH was performed with a telomere-PNA probe. After acquisition and constrained iterative deconvolution, all 3D nuclei were analyzed with TeloView to determine the numbers of telomeric signals per cell and telomere signal intensities, which were correlated with telomere length.

Figure 1A,B shows representative examples of 2D and 3D telomere (red) organization in a nucleus (blue). Figure 1C is a scatterplot that illustrates the number of telomere signals at a specific intensity of 100 nuclei per sample. From the 3D telomere profiles, we compared a normal epithelial sample with a tumor sample obtained from each patient and then analyzed the data for all 16 patients.

Normal esophageal epithelium versus ESCC

TeloView indicated the presence of different numbers of telomeres in the normal epithelial and tumor cells. Figure 2A shows the differences in telomere numbers for each patient, and Figure 2B shows the sums for the 16 patients. The mean for the normal epithelial telomeres was 27.95 (standard error [SE] = 0.77), whereas that for the tumor telomeres was 22.12 (SE = 0.77). This difference is statistically significant ($P < 0.0001$).

TeloView also indicated the differences in the total telomere intensities between the normal epithelial and tumor cells. Figure 3A,B shows the differences in the total telomere intensities for each patient and the sums for the 16 patients. The mean of the total telomere intensities in the normal epithelial samples was 208,411.27 a.u. (SE = 9718.41), whereas that in the tumor samples was 165,692.34 a.u. (SE = 9766.47). This difference is statistically significant ($P = 0.0078$).

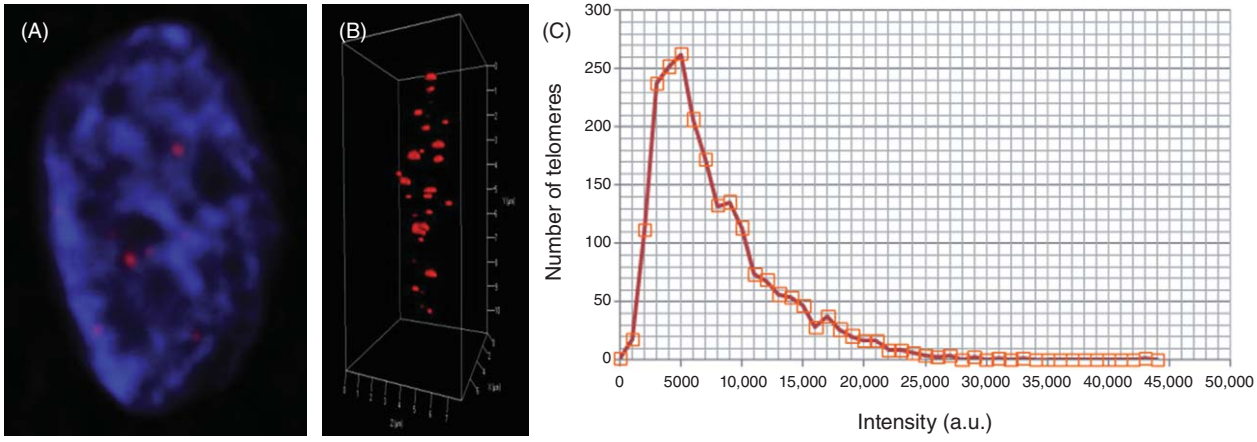

Fig. 1 (A) 2D and (B) 3D view of Q-FISH of ESCC nucleus (blue) and telomeres (red). (C) Graph distribution of number of telomeres according to their intensity (length of telomeres) for 100 cells from one sample.

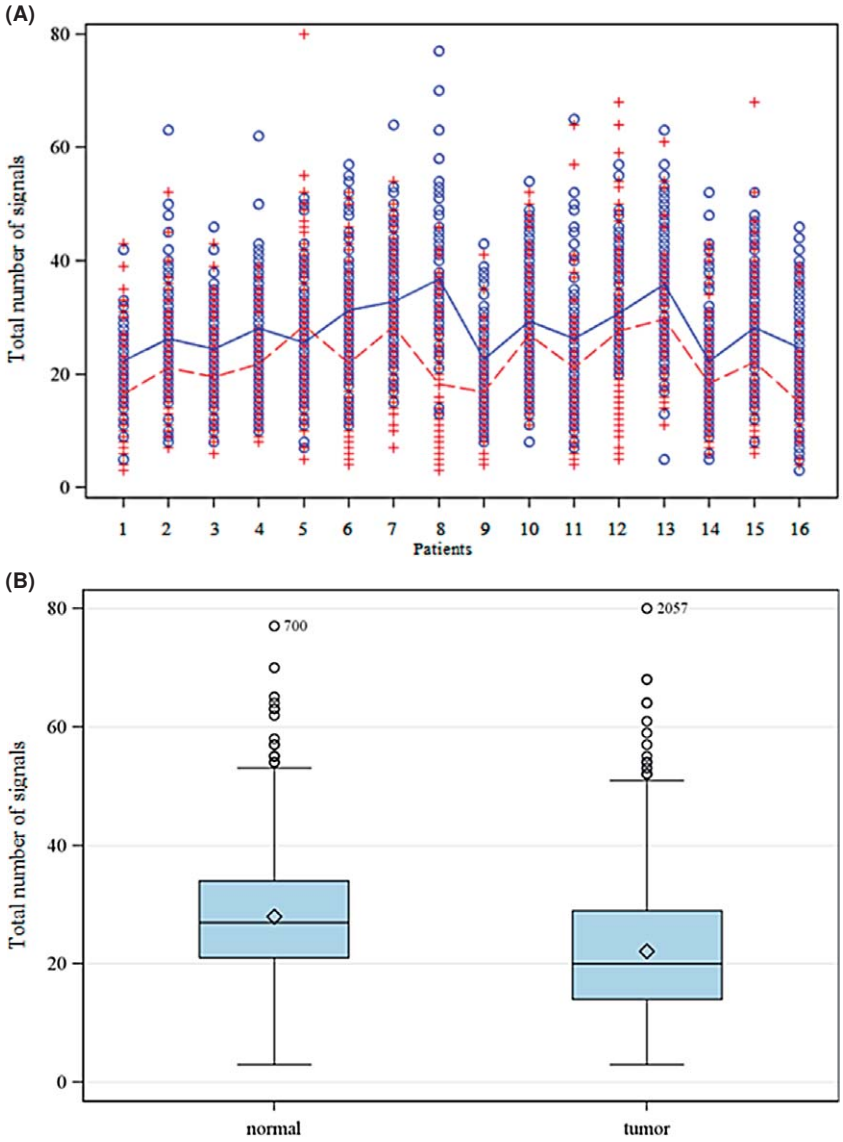

Fig. 2 (A) Graphs of number of telomeres between normal epithelium and tumor in each patient. (—o—) Normal, (- - + - -) tumor. (B) The sum of number of telomeres in total 16 patients.

We also analyzed the average intensity of all signals. The mean of the average intensity of all signals in the normal epithelial cells was 7444.03 a.u. (SE = 356.83), whereas that in the tumor cells was 7579.54 a.u. (SE = 358.60). This difference is not statistically significant ($P = 0.79$).

We did not find a significant difference in telomere aggregates between the normal epithelial and tumor cells; The mean of the normal epithelial nuclear volume was 233.29 μm^3 (SE = 10.55), and that for the tumor samples was 201.67 μm^3 (SE = 10.60), which is not a statistically significant difference ($P = 0.16$).

Young age versus old age

There were eight patients in the young age group (38–45 years old) and another eight patients in the old age group (81–93 years old). There were no statistically significant differences between the young and old age groups with regard to the number of telomeres, total intensity, average intensity of all signals or nuclear volume (Table 1).

ALT pathway in ESCC

We observed strong anti-PML signals on the positive control slides for the U2OS cell line (Fig. 4A), whereas no signals were detected on the slides containing the normal epithelial and ESCC tissues (Fig. 4B,C).

DISCUSSION

ESCC is a cancer of the esophageal epithelial layer that rapidly proliferates. There is a limited understanding of the differences between the telomere architectures of cancer cells and normal epithelial

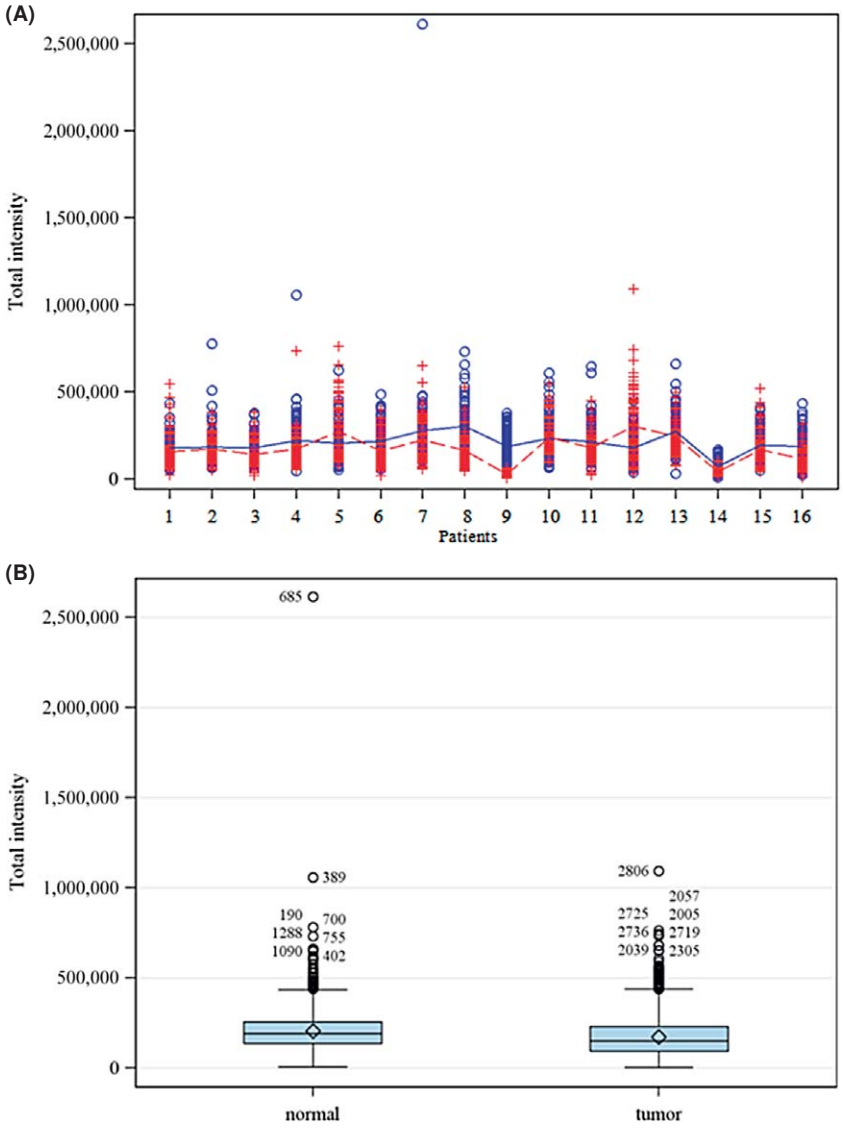

Fig. 3 (A) Graphs of total intensities of telomeres between normal epithelium and tumor in each patient. (—o—) Normal, (- - + - -) tumor. (B) The sum of total intensities of telomeres in total 16 patients.

cells. Our previous data have shown altered 3D telomeric organization in cervical cancer, glioblastoma, head and neck cancer, and thyroid cancer.[10,12,16,19,26] Thus, we investigated whether there was a difference in 3D nuclear telomere architecture between normal esophageal epithelial cells and esophageal cancer cells and also between young- and old-aged patients.

Table 1 The parameters of three-dimensional telomere architecture comparing young- and old-aged patients

	Young (SE)	Old (SE)	*P*-value
Number of telomere			0.88
Normal	27.30 (2.07)	28.54 (2.11)	
Tumor	21.82 (2.10)	22.44 (2.11)	
Total intensity (a.u.)			0.45
Normal	184,103.25 (27,554.69)	228,765.51 (28,083.73)	
Tumor	173,474.29 (27,843.31)	174,916.22 (28,101.37)	
Average intensity (a.u.)			0.47
Normal	6,958.62 (788.96)	7,972.54 (804.10)	
Tumor	7,858.00 (797.22)	7,711.26 (804.61)	
Nuclear volume (μm^3)			0.81
Normal	233.68 (35.31)	211.94 (35.99)	
Tumor	204.50 (35.68)	199.45 (36.01)	

μm^3, Micron; a.u., arbitrary; SE, standard error.

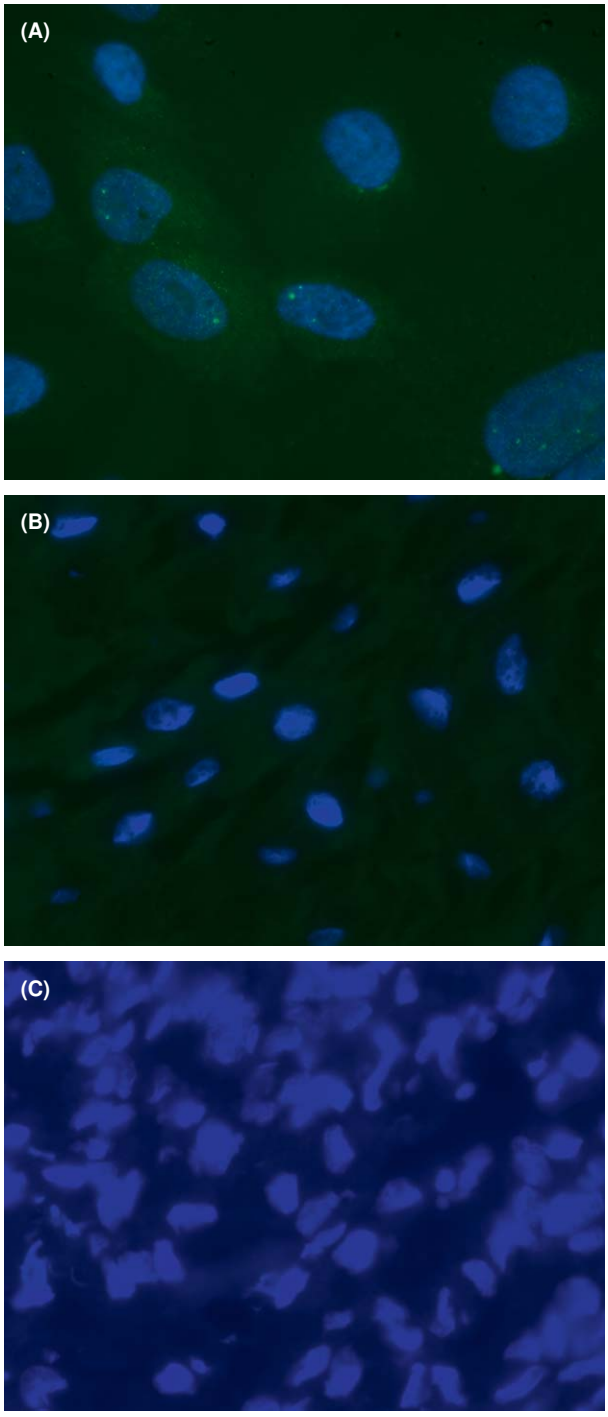

Fig. 4 (A) Green fluorescent signals of anti-promyelocytic leukemia (PML) on the positive control cell line. (B) No anti-PML signal on the normal esophageal epithelium. (C) No anti-PML signal on the esophageal squamous cell carcinoma.

Normal esophageal epithelium versus ESCC

We analyzed the 3D nuclear telomere architecture and determined the telomere numbers, telomere signal intensities, nuclear volumes, and the presence of telomere aggregates in the normal esophageal epithelial cells and ESCC cells. Using these parameters, we determined the 3D telomeric profiles and were able to differentiate between the normal esophageal epithelial and ESCC cells.

Our analysis of the evolution of telomere dysfunction in ESCC showed that the number of telomeres in the ESCC cells was less than that in the normal epithelial cells. This may be explained by the fact that some telomeres in cancer cells are too short to be detected because some studies have reported that ESCC telomeres are shorter than those in normal epithelium.[27,28]

To assess the length of telomeres, we measured the intensity of telomere signals and found that the total intensity of these signals in the ESCC cells was less than that in the normal epithelial cells. However, when we analyzed the average intensity of all signals, there were no differences between the ESCC and normal epithelial cells. These results may be explained by the fact that some telomeres in tumor cells form aggregates with greater than normal intensity levels. Thus, we did not see any differences in average telomere length in the tumor cells compared with the normal cells.

Telomere aggregates are clusters of telomeres that are fused or telomeres in close proximity that cannot be further resolved into separate signals (telomeres) at 200 mm. We have previously identified telomere aggregates as specific signatures of tumor cells.[10,12] These aggregates are features of tumor cells, a higher number of which reflects ongoing genomic instability.[29] We found increased telomere aggregates in the cancer tissues of 8 out of a total of 16 patients. The other eight patients had increased numbers of telomere aggregates in their normal epithelial tissues. These results may be explained by the fact that some short and especially critically shortened telomeres in cancer tissues may form aggregates, but are not classified as telomere aggregates by software because their cumulative intensity falls below the threshold level for the fluorescence intensity of telomeres.

For the nuclear volume assessment, we did not see any differences between the cancer cells and normal epithelial cells. Based on these data, differences in telomere architecture were present in the tumor cells versus the normal epithelial cells.

Young versus old patients

For the clinical portion of this study, we compared 3D telomere architecture in the young age group versus that in the old age group. We did not observe any differences in the number of telomeres, total intensities of telomere signals, average intensity of all signals or nuclear volume. The data showed a homogeneous population of telomeres between the young and old patients. These findings may provide valuable information for the development of telomere-targeted therapy in the future.

ALT pathway in ESCC

Telomerase plays a major role in telomere lengthening in rapidly dividing cells, such as tumor cells.[7] The recombination-based alternative lengthening pathway, termed ALT, also plays a role in telomere maintenance. In contrast with cells with active telomerase, those that use ALT possess APBs.[24,25] Our study showed no role of the ALT pathway in ESCC. These results correlate with a previous study reporting ALT negativity in ESCC.[30]

CONCLUSIONS

3D telomere Q-FISH was able to detect differences in telomere architecture between ESCC and normal epithelial cells; however, no differences were observed between the young and old patients.

Acknowledgments

The authors thank Mary Chuang (Genomic Center for Cancer Research and Diagnosis, Manitoba Institute of Cell Biology, University of Manitoba, Winnipeg, Manitoba, Canada) for her assistance with the statistical analyses, Alexandra Kuzyk (Genomic Center for Cancer Research and Diagnosis, Manitoba Institute of Cell Biology, University of Manitoba, Winnipeg, Manitoba, Canada) for reviewing the manuscript and the patients who made this study feasible. This study was supported by the Canadian Institutes of Health Research (S.M.) and Prince of Songkla University (S.S.).

References

1 Parkin D M, Bray F, Ferlay J, Pisani P. Global cancer statistics, 2002. CA Cancer J Clin 2005; 55: 74–108.
2 Kamangar F, Dores G M, Anderson W F. Patterns of cancer incidence, mortality, and prevalence across five continents: defining priorities to reduce cancer disparities in different geographic regions of the world. J Clin Oncol 2006; 24: 2137–50.
3 de Lange T. Shelterin: the protein complex that shapes and safeguards human telomeres. Genes Dev 2005; 19: 2100–10.
4 Gadji M, Vallente R, Klewes L *et al*. Nuclear remodeling as a mechanism for genomic instability in cancer. Adv Cancer Res 2011; 112: 77–126.
5 Begus-Nahrmann Y, Hartmann D, Kraus J *et al*. Transient telomere dysfunction induces chromosomal instability and promotes carcinogenesis. J Clin Invest 2012; 122: 2283–8.
6 Harley C B, Futcher A B, Greider C W. Telomeres shorten during ageing of human fibroblasts. Nature 1990; 345: 458–60.
7 Zvereva M I, Shcherbakova D M, Dontsova O A. Telomerase: structure, functions, and activity regulation. Biochemistry 2010; 75: 1563–83.
8 Blackburn E H. Switching and signaling at the telomere. Cell 2001; 106: 661–73.
9 Cesare A J, Reddel R R. Alternative lengthening of telomeres: models, mechanisms and implications. Nat Rev Genet 2010; 11: 319–30.
10 Chuang T C, Moshir S, Garini Y *et al*. The three-dimensional organization of telomeres in the nucleus of mammalian cells. BMC Biol 2004; 2: 12.
11 Mai S, Garini Y. Oncogenic remodeling of the three-dimensional organization of the interphase nucleus: c-Myc induces telomeric aggregates whose formation precedes chromosomal rearrangements. Cell Cycle 2005; 4: 1327–31.
12 Mai S, Garini Y. The significance of telomeric aggregates in the interphase nuclei of tumor cells. J Cell Biochem 2006; 97: 904–15.
13 Louis S F, Vermolen B J, Garini Y *et al*. c-Myc induces chromosomal rearrangements through telomere and chromosome remodeling in the interphase nucleus. Proc Natl Acad Sci U S A 2005; 102: 9613–8.
14 Kuzyk A, Mai S. Selected telomere length changes and aberrant three-dimensional nuclear telomere organization during fast-onset mouse plasmacytomas. Neoplasia 2012; 14: 344–51.
15 Guffei A, Lichtensztejn Z, Gonçalves Dos Santos Silva A, Louis S F, Caporali A, Mai S. c-Myc-dependent formation of Robertsonian translocation chromosomes in mouse cells. Neoplasia 2007; 9: 578–88.
16 Guijon F B, Greulich-Bode K, Paraskevas M, Baker P, Mai S. Premalignant cervical lesions are characterized by dihydrofolate reductase gene amplification and c-Myc overexpression: possible biomarkers. J Low Genit Tract Dis 2007; 11: 265–72.
17 Knecht H, Sawan B, Lichtensztejn D, Lemieux B, Wellinger R J, Mai S. The 3D nuclear organization of telomeres marks the transition from Hodgkin to Reed–Sternberg cells. Leukemia 2009; 23: 565–73.
18 Guffei A, Sarkar R, Klewes L, Righolt C, Knecht H, Mai S. Dynamic chromosomal rearrangements in Hodgkin's lymphoma are due to ongoing three-dimensional nuclear remodeling and breakage–bridge–fusion cycles. Haematologica 2010; 95: 2038–46.
19 Gadji M, Fortin D, Tsanaclis A M *et al*. Three-dimensional nuclear telomere architecture is associated with differential time to progression and overall survival in glioblastoma patients. Neoplasia 2010; 12: 183–91.
20 Knecht H, Kongruttanachok N, Sawan B *et al*. Three-dimensional telomere signatures of Hodgkin– and Reed–Sternberg cells at diagnosis identify patients with poor response to conventional chemotherapy. Transl Oncol 2012; 5: 269–77.
21 Gadji M, Adebayo Awe J, Rodrigues P *et al*. Profiling three-dimensional nuclear telomeric architecture of myelodysplastic syndromes and acute myeloid leukemia defines patient subgroups. Clin Cancer Res 2012; 18: 3293–304.
22 Vermolen B J, Garini Y, Mai S *et al*. Characterizing the three-dimensional organization of telomeres. Cytometry A 2005; 67: 144–50.
23 Schaefer L H, Schuster D, Herz H. Generalized approach for accelerated maximum likelihood based image restoration applied to three-dimensional fluorescence microscopy. J Microsc 2001; 204 (Pt 2): 99–107.
24 Yu J, Lan J, Wang C *et al*. PML3 interacts with TRF1 and is essential for ALT-associated PML bodies assembly in U2OS cells. Cancer Lett 2010; 291: 177–86.
25 Wang C, Xiao H, Ma J *et al*. The F-box protein β-TrCP promotes ubiquitination of TRF1 and regulates the ALT-associated PML bodies formation in U2OS cells. Biochem Biophys Res Commun 2013; 434: 728–34.
26 Wark L, Danescu A, Natarajan S *et al*. Three-dimensional telomere dynamics in follicular thyroid cancer. Thyroid 2014; 24: 296–304.
27 Takubo K, Fujita M, Izumiyama N *et al*. Q-FISH analysis of telomere and chromosome instability in the oesophagus with and without squamous cell carcinoma in situ. J Pathol 2010; 221: 201–9.
28 Shiraishi H, Mikami T, Aida J *et al*. Telomere shortening in Barrett's mucosa and esophageal adenocarcinoma and its association with loss of heterozygosity. Scand J Gastroenterol 2009; 44: 538–44.
29 Mai S. Initiation of telomere-mediated chromosomal rearrangements in cancer. J Cell Biochem 2010; 109: 1095–102.
30 Heaphy C M, Subhawong A P, Hong S M *et al*. Prevalence of the alternative lengthening of telomeres telomere maintenance mechanism in human cancer subtypes. Am J Pathol 2011; 179: 1608–15.